Available online at www.sciencedirect.com

SCIENCE DIRECT®

Journal of Molecular Catalysis A: Chemical 200 (2003) 81–94

JOURNAL OF MOLECULAR CATALYSIS A: CHEMICAL

www.elsevier.com/locate/molcata

Synthesis of new *o*-alkyl substituted arylalkylphosphanes: study of their molecular structure and influence on rhodium-catalyzed propene and 1-hexene hydroformylation

Helena Riihimäki [a,*], Teija Kangas [a], Pekka Suomalainen [b], Heidi K. Reinius [c], Sirpa Jääskeläinen [b], Matti Haukka [b], A.O.I. Krause [c], Tapani A. Pakkanen [b], Jouni T. Pursiainen [a]

[a] *Department of Chemistry, University of Oulu, P.O. Box 3000, FIN-90014 Oulu, Finland*
[b] *Department of Chemistry, University of Joensuu, P.O. Box 111, FIN-80101 Joensuu, Finland*
[c] *Department of Chemical Technology, Helsinki University of Technology, P.O. Box 6100, FIN-02015 HUT, Finland*

Received 6 November 2002; received in revised form 8 November 2002; accepted 11 November 2002

Abstract

A set of new phosphane ligands designed to increase the branched-to-normal ratio of the hydroformylation reaction were prepared in the same way as the previously reported *ortho*-alkyl substituted arylphosphanes, which have shown increased *i*/*n* ratios in the hydroformylation of propene and 1-hexene. In order to determine the relationship between the catalytic behavior and stereoelectronic properties of the ligands, various functional alkyl groups (methyl, isopropyl, cyclohexyl) were placed on the phosphorus atom directly and in the *ortho* position of the phenyl ring connected to phosphorus. In the hydroformylation reaction of propene and 1-hexene a higher *i*/*n* ratio resulted with nearly all the ligands compared with that of triphenylphosphane. Additionally as the *ortho*-alkyl-substituent became larger, it had a favorable effect on the *i*-selectivity. Characterization of the ligands was carried out by NMR spectroscopy (mainly ^{1}H, $^{31}P\{^{1}H\}$, $^{13}C\{^{1}H\}$, HSQC/HETCOR and COSY-90). Properties of the ligands were also studied by quantum mechanical calculations and by synthesizing three Rh(acac)(CO)(PR_3) derivatives. The *o*-alkyl-substituent was orientated outside the ligands' cone angle in the X-ray crystal structures of (2-cyclohexylphenyl)dicyclohexylphosphane and (2,5-dimethylphenyl)bis(4-pyridyl)phosphane, and Rh(acac)(CO)(PR_3) complex of (2-methylphenyl)dicyclohexylphosphane.

Keywords: Hydroformylation; Phosphane; Alkyl groups; NMR spectroscopy; Ab initio calculations

1. Introduction

Catalytic hydroformylation of olefins is an important process in the petrochemical and the fine chemicals industries. Improved isomer ratios, milder reaction conditions and higher activities are the significant advantages of phosphane-modified rhodium-catalysts [1–3]. Both the electronic and steric properties of the catalysts can be greatly affected by an appropriate choice of phosphane ligands. Despite numerous studies, however, the demanding question how phosphorus ligands control the selectivity of hydroformylation still awaits solution [4].

* Corresponding author. Tel.: +358-8-553-1647; fax: +358-8-553-1603.
E-mail address: helena.riihimaki@oulu.fi (H. Riihimäki).

1381-1169/03/$ – see front matter © 2003 Elsevier Science B.V. All rights reserved.
doi:10.1016/S1381-1169(03)00026-8

Producing linear *n*-butanal regioselectively has been the goal in the most important industrial hydroformylation process, propene hydroformylation, for a long time [1–3,5]. Recently, interest in selective formation of the branched form, isobutanal, used in the production of polyols, such as neopentyl glycol has increased [5]. Earlier, higher iso-to-normal (*i*/*n*) product ratios and greater activity in hydroformylation have been observed as the bulkier *ortho*-substituted triarylphosphite (e.g. tris(*o*-phenoxyphenyl)phosphite and tris(*o*-*tert*-butylphenyl)phosphite) have been used as ligands [6–10]. It has been suggested that bulky ligands favor low coordination numbers, and thus, the coordinative unsaturation of the metal center becomes greater favoring branched products [7–12].

Similar results have been observed with bulky arylphosphanes. The activity of the 1-butene hydroformylation reaction and *i*-selectivity of 2-butene hydroformylation have become greater as catalysts have been modified with *o*-substituted arylphosphanes [13,14]. Moreover, in the hydroformylation of propene, we have achieved enhanced selectivity to branched aldehydes by using *o*-alkyl substituted triphenylphosphane with rhodium catalysts [5,15]. The activity and selectivity of these catalysts is attributable to the stereochemistry and large cone angle of the bulky phosphane ligands [8,9,12].

Rhodium complexes of strongly basic trialkylphosphanes (greater σ-electron donor ability) are more stable and less active low-pressure hydroformylation catalysts than weakly basic triarylphosphane complexes at comparable temperatures [16,17]. However, the *i*/*n* selectivity of alkylphosphane complexes and the equilibria between the major carbonylhydride complexes are very much dependent on the site and the degree of their branching (i.e. steric crowding in the vicinity of their P atoms) [16]. In the cobalt-catalyzed hydroformylation of 1-hexenes bulkier tris(*i*-propyl)-phosphane has showed higher *i*/*n* ratios than tris(*n*-propyl)phosphane [12]. Alkyldiphenylphosphane ligands branched at their α- or β-alkyl carbon atoms, including cyclohexyldiphenylphosphane, have been found to form bis(phosphane)—rather than tris(phosphane)-carbonylhydridorhodium complexes under simulated hydroformylation conditions. As a consequence, they were more active catalyst ligands for hydroformylation and led to the formation of aldehyde products having higher *i*/*n* isomer ratios [16].

After the results of our previous study with *o*-methyl, *o*-ethyl, *o*-isopropyl and *o*-cyclohexyl substituted arylphosphanes we have prepared seven new arylalkylphosphanes: (2-methylphenyl)diisopropylphosphane (**1**), (2-cyclohexylphenyl)diisopropylphosphane (**2**), bis(2-methylphenyl)isopropylphosphane (**3**), (2-methylphenyl)dicyclohexylphosphane (**4**), (2-cyclohexylphenyl)dicyclohexylphosphane (**5**), (2-methylnaphthyl)diisopropylphosphane (**6**) and (2-methylnaphthyl)dicyclohexylphosphane (**7**) [5,15,18]. Moreover, new *o*-alkyl substituted pyridylphosphanes (2,5-dimethylphenyl)bis(3-pyridyl)phosphane (**8**) and (2,5-dimethylphenyl)bis(4-pyridyl)phosphane (**9**) have also been prepared since pyridylphosphane-based catalysts have earlier shown higher reaction rates than PPh_3 [19,20]. Characterization of the ligands was made by NMR spectroscopy. The ligands were tested in the hydroformylation of propene and 1-hexene.

Three Rh(acac)(CO)(PR_3) complexes: Rh(acac)-(CO)(**3**), Rh(acac)(CO)(**4**) and Rh(acac)(CO)(**5**) in a reaction between Rh(acac)$(CO)_2$ and phosphane (PR_3) were prepared and characterized in order to investigate the coordination properties of the ligands and orientation of the *o*-alkyl-substituents. Geometrical arrangement and steric size (cone angle) of the free and coordinated ligands were studied theoretically by ab initio Hartree–Fock and DFT methods. Crystal structures for ligands (2-cyclohexylphenyl)dicyclohexylphosphane (**5**) and (2,5-dimethylphenyl)bis(4-pyridyl)phosphane (**9**), and Rh(acac)(CO)(**4**) complex were determined as well.

2. Experimental section

General comments: The phosphanes are air- and moisture-sensitive, both as pure compounds and in solution, and unprotected show observable oxidation within one day. Thus, all reactions were carried out with standard Schlenk techniques under nitrogen or argon atmosphere. The new arylalkylphosphanes (**1**–**9**) studied in this work (Scheme 1) were prepared by modified literature methods from *ortho*-substituted brominated aromatics by lithiation with *n*-butyllithium and further reaction with chloroalkylphosphanes or dichloro(2,5-dimethylphenyl)phosphane [21,22]. The dichloro(2,5-dimethylphenyl)phosphane used in the synthesis of pyridylphosphanes was prepared by

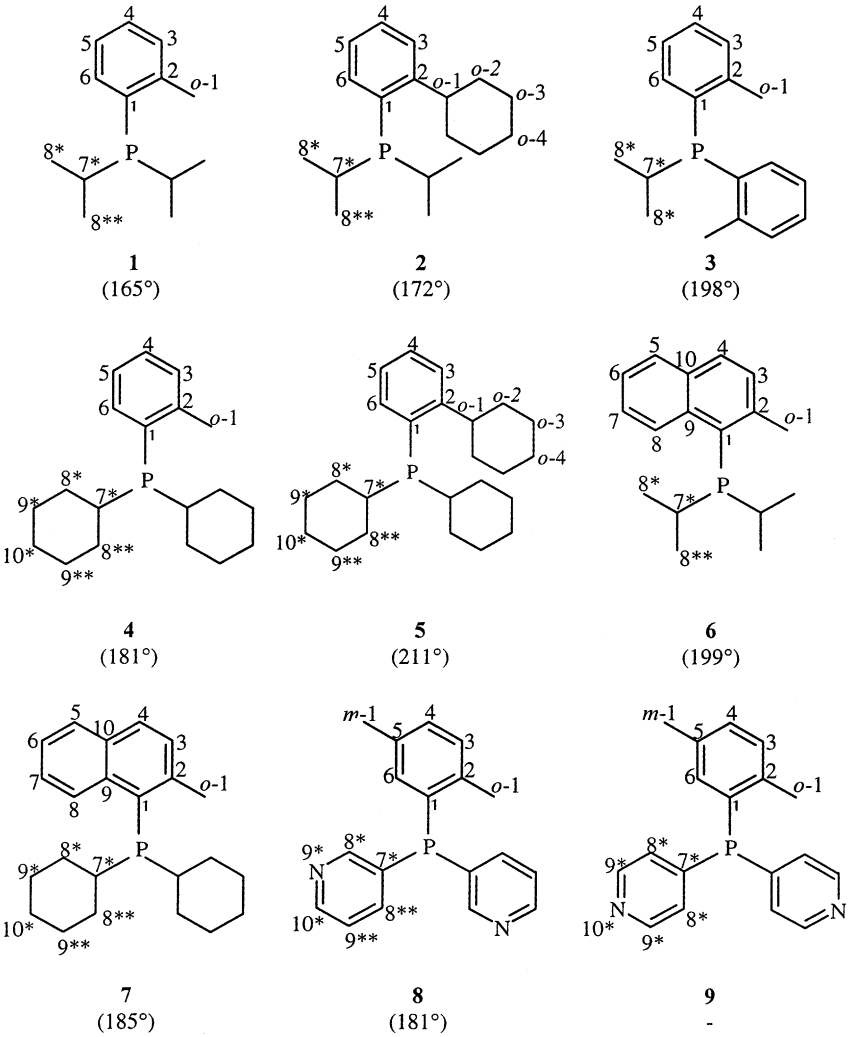

Scheme 1. Schematic structures and cone angles of reported ligands.

Friedel–Crafts reaction of phosphorus trichloride with *p*-xylene in the presence of aluminium chloride as catalyst [23]. 2-Bromotoluene (99%), 1-bromo-2-methylnaphthalene (tech., 90%), 3-bromopyridine (99%), 4-bromopyridine hydrochloride (99%), chlorodiisopropylphosphane (96%), chlorodicyclohexylphosphane (97%), dichloroisopropylphosphane (97%), *n*-butyllithium (2.5 M solution in hexane) and TMEDA (>99%) were obtained from Aldrich. 1-Bromo-2-cyclohexylbenzene (97%) was from Lancaster. Diethyl ether was distilled over sodium-benzophenone ketyl under nitrogen before use.

Characterization: The characterization of the ligands was based on ^{1}H-, ^{13}C{^{1}H}-, ^{31}P{^{1}H}-, H,H-correlated COSY-90-, H,C-correlated HSQC- or C,H-correlated HETCOR-NMR spectroscopy. Long-range C,H-correlated COLOC-NMR spectra were measured for ligands **1**, **3**, **5** and **6**. NMR spectra were recorded on Bruker DPX400 and AM200 spectrometers at room temperature in $CDCl_3$ (D 99.8%, 0.03% TMS). NMR spectra of the metal complexes were recorded on a Bruker AM250 spectrometer. ^{1}H-NMR: reference $SiMe_4$. ^{13}C{^{1}H}-NMR: $CDCl_3$ set to 77.0 ppm. ^{31}P{^{1}H}-NMR: external standard 85% H_3PO_4.

Table 1
$^{13}C\{^1H\}$ NMR (100 MHz) chemical shifts (ppm)[a] and coupling constants of doublets (Hz) for reported ligands **1**–**9**[b]

	1	**2**	**3**	**4**	**5**	**6**	**7**	**8**	**9**
C^{0-4}	–	26.28	–	–	26.38	–	–	–	–
C^{0-3}	–	26.80	–	–	26.89	–	–	–	–
C^{0-2}	–	34.40	–	–	34.58	–	–	–	–
C^{0-1}	22.04	40.88	21.45	22.29	41.09	24.53	22.61	21.35	20.74
$^3J_{CP}$	(24.9)	(26.4)	(22.0)	(22.2)	(26.1)	(27.4)	–	(21.4)	(22.2)
C^{m-1}	–	–	–	–	–	–	–	21.65	20.94
C^{10*}	–	–	–	26.36	26.48	–	26.36	151.77	–
C^{9*c}	–	–	–	27.05	27.16	–	27.04	–	149.67
$^3J_{CP}$	–	–	–	(9.2)	(7.0)	–	(8.4)	–	(5.0)
C^{9**c}	–	–	–	27.16	27.31	–	26.87	125.49	–
$^3J_{CP}$	–	–	–	(12.9)	(11.6)	–	(13.0)	(4.2)	–
C^{8*c}	19.33	19.28	19.73	28.97	29.28	21.18	30.49	155.65	127.83
$^2J_{CP}$	(11.1)	(11.1)	(20.6)	(7.3)	(8.4)	(14.3)	(10.7)	(25.4)	(16.5)
C^{8**c}	20.21	20.28	–	30.33	30.76	22.96	33.54	142.60	–
$^2J_{CP}$	(18.7)	(19.3)	–	(14.4)	(17.0)	(28.6)	(24.8)	(16.0)	–
C^{7*}	24.10	24.17	25.38	∼33.7[d]	∼34.5[e]	25.50	35.84	133.07	145.80
$^1J_{CP}$	(12.7)	(12.6)	(8.0)	–	–	(13.8)	(13.2)	(14.6)	(17.4)
C^5	125.08	124.90	125.75	125.28	124.92	128.96	129.25	134.70	131.14
C^4	128.39	128.65	128.23	129.04	128.74	129.73	129.74	131.83	131.01
$^4J_{CP}$	–	–	–	(3.0)	–	–	–	–	–
C^3	130.11	125.94	129.94	130.48	126.05	129.25	129.31	132.07	130.54
$^3J_{CP}$	(5.1)	(3.4)	(4.6)	(4.8)	(5.2)	(5.2)	–	(4.2)	(5.9)
C^6	132.35	132.23	131.54	132.88	132.69	124.47	124.52	134.51	133.72
$^2J_{CP}$	(2.2)	–	–	–	–	–	–	–	–
C^1	134.54	133.04	136.57	∼132.9[e]	∼132.7[e]	∼137.0[d]	∼136.5[d]	137.37	136.16
$^1J_{CP}$	(18.9)	(16.6)	(14.2)	–	–	–	–	–	–
C^2	144.76	154.73	142.97	145.05	155.05	∼145.0[d]	∼146.1[d]	140.40	140.02
$^2J_{CP}$	(26.6)	(23.2)	(25.6)	(24.2)	(23.6)	–	–	(26.7)	(27.4)
C^7	–	–	–	–	–	125.58	125.64	–	–
C^8	–	–	–	–	–	127.13	∼128.9[d]	–	–
$^3J_{CP}$	–	–	–	–	–	(9.7)	–	–	–
C^9	–	–	–	–	–	132.16	∼129.7[e]	–	–
$^2J_{CP}$	–	–	–	–	–	(26.9)	–	–	–
C^{10}	–	–	–	–	–	132.80	132.69	–	–

[a] Resonance peaks are singlets if no coupling constant are reported.
[b] Carbon atoms are numbered as in Scheme 1.
[c] Carbon atoms in pairs 8∗, 8∗∗ and 9∗, 9∗∗ are diastereotopic and thus non-equivalent with respect to P–C couplings and chemical shifts.
[d] Chemical shift can not be interpreted precisely because the resonance peak is broad and thus it is also impossible to interpret the multiplicity.
[e] Resonance peak can not be interpreted precisely because of overlapping and thus it is also impossible to interpret the multiplicity.

(2,5-Dimethylphenyl)bis(3-pyridyl)phosphane (**8**) was recorded at room temperature in acetone-d_6 (D 99.9%) because of solubility problems. ^{1}H-NMR: CD_3COCD_3 set to 2.05 ppm and $^{13}C\{^1H\}$-NMR: CD_3COCD_3 set to 30.5 ppm. $^{13}C\{^1H\}$-NMR shifts of free ligands are presented in Table 1. Exact mass peaks of the free ligands were determined on a Micromass LCT, using an ESI+ method. IR measurements of the metal complexes were done with a Nicolet 750 spectrometer in THF. The X-ray diffraction data were collected with a Nonius KappaCCD diffractometer.

2.1. Synthetic procedure for arylalkylphosphanes

A solution of *n*-butyllithium was transferred dropwise *via* a canula to a freshly prepared solution of

1-bromo-2-alkylbenzene or 1-bromo-2-methylnaphthalene in diethyl ether (30 ml) at −10 → 0 °C (salted ice bath). After stirring for 2 h at −10 → 0 °C, a solution of chlorodialkyl- or dichloroalkyl-phosphane in diethyl ether (25 ml) was slowly added to the bright mixture of *ortho*-substituted lithiated aromatics. Stirring was continued for a further 2 h at −10 → 0 °C. After slow warming to room temperature, some solid material precipitated (inorganic salts). Solid and liquid layers were separated by filtration and the solvent was removed in vacuo. A crude product was obtained from the solvent phase and purified by recrystallization (from ethanol or hexane) or by column chromatography using dichloromethane/hexane (1:2) as an eluent. The pure product was a bright viscous oil or a white solid.

*2.1.1. (2-Methylphenyl)diisopropylphosphane (**1**)*

Following the procedure described above, reactions of 2-bromotoluene (3.4 g, 2.4 ml, 20.0 mmol), *n*-butyllithium (8.0 ml, 20.0 mmol) and chlorodiisopropylphosphane (3.1 g, 3.2 ml, 20.0 mmol) afforded a crude yellow oily product. The general procedure was followed except the mixture was stirred over night to complete reaction. The crude yellow oily product was purified by column chromatography using dichloromethane/hexane (1:2) as an eluent. The yield of the pure bright oily product was 1.5 g, 7.1 mmol, 35%. ^{1}H NMR (200 MHz, $CDCl_3$, see Scheme 1 for numbering) δ_H (ppm): 0.91 (dd, $^{3}J_{HH}$ = 7.0 Hz, $^{3}J_{HP}$ = 11.6 Hz, H^{8*}, 6 H), 1.12 (dd, $^{3}J_{HH}$ = 7.0 Hz, $^{3}J_{HP}$ = 14.8 Hz, H^{8**}, 6 H), 2.11 (dsep, $^{3}J_{HH}$ = 7.0 Hz, $^{2}J_{HP}$ = 2.0 Hz, H^{7*}, 2 H), 2.57 (s, H^{0-1}, 3 H), 7.16 (m, H^{5}, 1 H), 7.18–7.23 (m, H^{3} and H^{4}, 2 H), 7.37 (m, H^{6}, 1 H). ^{31}P{^{1}H} NMR (161 MHz, $CDCl_3$) δ_P (ppm): −4.8. Exact mass (Micromass LCT, ESI+): 209.1466 $(M + H)^+$ (calcd. for $C_{13}H_{22}P$, 209.1459).

*2.1.2. (2-Cyclohexylphenyl)diisopropylphosphane (**2**)*

Reactions of 1-bromo-2-cyclohexylbenzene (2.8 g, 11.7 mmol), *n*-butyllithium (4.7 ml, 11.7 mmol) and chlorodiisopropylphosphane (1.8 g, 1.9 ml, 11.7 mmol) afforded a crude muddy and oily product. The bright oily product was obtained by washing the crude product with hexane several times; a white solid impurity was precipitated. The yield of the pure bright oily product was 2.7 g, 9.9 mmol, 84%. ^{1}H NMR (400 MHz, $CDCl_3$, see Scheme 1 for numbering) δ_H (ppm): 0.89 (dd, $^{3}J_{HH}$ = 7.2 Hz, $^{3}J_{HP}$ = 11.6 Hz, H^{8*}, 6 H), 1.14 (dd, $^{3}J_{HH}$ = 7.2 Hz, $^{3}J_{HP}$ = 14.8 Hz, H^{8**}, 6 H), 1.20–1.30 (m, H^{0-4}, 2 H), 1.36–1.48 (m, H^{0-2}, 4 H), 1.78 (m, H^{0-3}, 4 H), 2.08 (dsep, $^{3}J_{HH}$ = 7.0 Hz, $^{2}J_{HP}$ = 2.0 Hz, H^{7*}, 2 H), 3.68 (m, H^{0-1}, 1 H), 7.14 (m, H^{5}, 1 H), 7.27–7.30 (m, H^{3} and H^{4}, 2 H), 7.38 (m, H^{6}, 1 H). ^{31}P{^{1}H} NMR (161 MHz, $CDCl_3$) δ_P (ppm): −4.4. Exact mass (Micromass LCT, ESI+): 277.2060 $(M + H)^+$ (calcd. for $C_{18}H_{30}P$, 277.2085).

*2.1.3. Bis(2-methylphenyl)isopropylphosphane (**3**)*

Reactions of 2-bromotoluene (11.8 g, 4.2 ml, 34.5 mmol), *n*-butyllithium (13.8 ml, 34.5 mmol) and dichloroisopropylphosphane (2.5 g, 2.1 ml, 17.2 mmol) afforded a bright oily product, which was dissolved in ethanol and filtered over silica. The yield of the pure bright oily product was 3.6 g, 14.0 mmol, 81%. ^{1}H NMR (400 MHz, $CDCl_3$, see Scheme 1 for numbering) δ_H (ppm): 1.11 (dd, $^{3}J_{HH}$ = 6.8 Hz, $^{3}J_{HP}$ = 15.9 Hz, H^{8*}, 6 H), 2.40 (m, H^{7*}, 1 H), 2.45 (s, H^{0-1}, 6 H), 7.10–7.20 (m, H^{3}, H^{4} and H^{5}, 6 H), 7.30 (m, H^{6}, 2 H). ^{31}P{^{1}H} NMR (161 MHz, $CDCl_3$) δ_P (ppm): −22.3. Exact mass (Micromass LCT, ESI+): 257.1432 $(M + H)^+$ (calcd. for $C_{17}H_{22}P$, 257.1459).

*2.1.4. (2-Methylphenyl)dicyclohexylphosphane (**4**)*

Reactions of 2-bromotoluene (2.6 g, 1.8 ml, 15.0 mmol), *n*-butyllithium (6.0 ml, 15.0 mmol) and chlorodicyclohexylphosphane (3.5 g, 3.3 ml, 15.0 mmol) afforded a white solid product, which was recrystallized from ethanol. The yield of the pure white solid product was 3.6 g, 12.4 mmol, 82%. ^{1}H NMR (400 MHz, $CDCl_3$, see Scheme 1 for numbering) δ_H (ppm): 1.00–2.00 (m, H^{7*}, H^{8*}, H^{8**}, H^{9*}, H^{9**}, H^{10*}, 22 H), 2.56 (s, H^{0-1}, 3 H), 7.15–7.25 (m, H^{3}, H^{4} and H^{5}, 3 H), 7.38 (m, H^{6}, 1 H). ^{31}P{^{1}H} NMR (161 MHz, $CDCl_3$) δ_P (ppm): −11.6. Exact mass (Micromass LCT, ESI+): 289.2084 $(M + H)^+$ (calcd. for $C_{19}H_{30}P$, 289.2085).

*2.1.5. (2-Cyclohexylphenyl)dicyclohexylphosphane (**5**)*

Reactions of 1-bromo-2-cyclohexylbenzene (5.1 g, 21.5 mmol), *n*-butyllithium (8.6 ml, 21.5 mmol) and chlorodicyclohexylphosphane (5.0 g, 4.7 ml, 21.5 mmol) afforded a white solid product, which was recrystallized from ethanol. The yield of the pure white

solid product was 5.8 g, 16.4 mmol, 76%. ^{1}H NMR (400 MHz, $CDCl_3$, see Scheme 1 for numbering) δ_H (ppm): 1.00–1.95 (m, H^{0-2}, H^{0-3}, H^{0-4}, H^{7*}, H^{8*}, H^{8**}, H^{9*}, H^{9**}, H^{10*}, 32 H), 3.66 (m, H^{0-1}, 1 H), 7.14 (m, H^5, 1 H), 7.27–7.31 (m, H^3 and H^4, 2 H), 7.40 (m, H^6, 1 H). $^{31}P\{^1H\}$ NMR (161 MHz, $CDCl_3$) δ_P (ppm): −14.6. Exact mass (Micromass LCT, ESI+): 357.2687 $(M + H)^+$ (calcd. for $C_{24}H_{38}P$, 357.2711).

2.1.6. (2-Methylnaphthyl)diisopropylphosphane (**6**)

Reactions of 1-bromo-2-methylnaphthalene (4.2 g, 2.9 ml, 18.9 mmol), *n*-butyllithium (7.6 ml, 18.9 mmol) and chlorodiisopropylphosphane (2.9 g, 3.0 ml, 18.9 mmol) afforded a crude reddish brown oily product. The crude product was purified by column chromatography using dichloromethane/hexane (1:2) as an eluent. The yield of the pure bright oily product was 2.0 g, 7.8 mmol, 41%. ^{1}H NMR (400 MHz, $CDCl_3$, see Scheme 1 for numbering) δ_H (ppm): 0.73 (dd, $^3J_{HH} = 6.8$ Hz, $^3J_{HP} = 13.8$ Hz, H^{8*}, 6 H), 1.32 (dd, $^3J_{HH} = 6.8$ Hz, $^3J_{HP} = 17.2$ Hz, H^{8**}, 6 H), 2.73 (broad, H^{7*}, 2 H), 2.82 (broad, H^{0-1}, 3 H), 7.29 (dd, $^3J_{HH} = 8.2$ Hz, $^4J_{HP} = 3.4$ Hz, H^3, 1 H), 7.37 (t, $^3J_{HH} = 7.4$ Hz, H^6, 1 H), 7.45 (t, $^3J_{HH} = 7.6$ Hz, H^7, 1 H), 7.70 (d, $^3J_{HH} = 8.4$ Hz, H^4, 1 H), 7.77 (d, $^3J_{HH} = 8.0$ Hz, H^5, 1 H), 8.24 (broad, H^8, 1 H). $^{31}P\{^1H\}$ NMR (161 MHz, $CDCl_3$) δ_P (ppm): 6.6. Exact mass (Micromass LCT, ESI+): 259.1632 $(M + H)^+$ (calcd. for $C_{17}H_{24}P$, 259.1616).

2.1.7. (2-Methylnaphthyl)dicyclohexylphosphane (**7**)

Reactions of 1-bromo-2-methylnaphthalene (3.2 g, 2.2 ml, 14.3 mmol), *n*-butyllithium (5.7 ml, 14.3 mmol) and chlorodicyclohexylphosphane (3.3 g, 3.2 ml, 14.3 mmol) afforded a crude yellowish oily product. The crude product was purified by column chromatography using dichloromethane/hexane (1:2) as an eluent. The yield of the pure bright oily product was 3.2 g, 9.4 mmol, 66%. ^{1}H NMR (400 MHz, $CDCl_3$, see Scheme 1 for numbering) δ_H (ppm): 0.88–2.10 (m, H^{8*}, H^{8**}, H^{9*}, H^{9**} and H^{10*}, 20 H), 2.52 (m, H^{7*}, 2 H), 2.84 (s, H^{0-1}, 3 H), 7.31 (d, $^3J_{HH} = 7.6$ Hz, H^3, 1 H), 7.40 (t, $^3J_{HH} = 7.4$ Hz, H^6, 1 H), 7.48 (t, $^3J_{HH} = 7.6$ Hz, H^7, 1 H), 7.72 (d, $^3J_{HH} = 8.4$ Hz, H^4, 1 H), 7.79 (d, $^3J_{HH} = 7.2$ Hz, H^5, 1 H), 8.19 (broad, H^8, 1 H). $^{31}P\{^1H\}$ NMR (161 MHz, $CDCl_3$) δ_P (ppm): −8.1. Exact mass (Micromass LCT, ESI+): 339.2251 $(M + H)^+$ (calcd. for $C_{23}H_{32}P$, 339.2242).

2.2. Synthetic procedure for pyridylphosphanes (**8**) and (**9**)

n-Butyllithium (12.0 ml, 30 mmol) was slowly added to dry TMEDA (4.6 ml, 30 mmol). The mixture was stirred for 15 min at room temperature and then cooled to −70 °C when cold ether (−70 °C, 75 ml) was added. This mixture was then cooled to −115 °C and bromopyridine (30 mmol, Aldrich, 99%) in diethyl ether (30 ml) was added dropwise. The mixture was stirred around 5 min, and then dichloro(2,5-dimethylphenyl)phosphane (10 mmol) was added [23]. After 30 min, the rest of dichloro(2,5-dimethylphenyl)phosphane (5 mmol) was added, and the yellow mixture was stirred for 2.5 h at −100 °C, before warming to room temperature overnight. The mixture was extracted with H_2SO_4 (2 M), and the aqueous layer was separated and made alkaline with NaOH. The white or light yellow solid product was obtained by extraction of the aqueous phase with diethyl ether. After extraction, the diethyl ether was removed in vacuo. The crude product was purified by column chromatography using dichloromethane/hexane/methanol (10:3:1) as an eluent. The yield of the pure white solid (2,5-dimethylphenyl)bis(3-pyridyl)phosphane (**8**) was 1.3 g, 4.5 mmol, 30%. ^{1}H NMR (400 MHz, CD_3COCD_3, see Scheme 1 for numbering) δ_H (ppm): 2.16 (s, H^{m-1}, 3 H), 2.34 (s, H^{0-1}, 3 H), 6.64 (m, H^6, 1 H), 7.19 (m, H^3, H^4, 2 H), 7.42 (m, H^{9**}, 2 H), 7.61 (m, H^{8**}, 2 H), 8.45 (m, H^{8*}, 2 H), 8.61 (m, H^{10*}, 2 H). $^{31}P\{^1H\}$ NMR (161 MHz, $CDCl_3$) δ_P (ppm): −25.0. Exact mass (Micromass LCT, ESI+): 293.1183 $(M + H)^+$ (calcd. for $C_{18}H_{18}N_2P$, 293.1208). The yield of the pure bright solid (2,5-dimethylphenyl)bis(4-pyridyl)phosphane (**9**) was 0.5 g, 1.8 mmol, 12%. ^{1}H NMR (400 MHz, $CDCl_3$, see Scheme 1 for numbering) δ_H (ppm): 2.19 (s, H^{m-1}, 3 H), 2.40 (s, H^{0-1}, 3 H), 6.59 (m, H^6, 1 H), 7.11–7.20 (m, H^3, H^4, H^{8*}, 6 H), 8.59 (m, H^{9*}, 4 H). $^{31}P\{^1H\}$ NMR (161 MHz, $CDCl_3$) δ_P (ppm): −15.7. Exact mass (Micromass LCT, ESI+): 293.1220 $(M + H)^+$ (calcd. for $C_{18}H_{18}N_2P$, 293.1208).

2.3. Synthetic procedure for Rh(acac)(CO)(PR_3) complexes

(Acetylacetonato)dicarbonylrhodium(I) (50 mg, 0.19 mmol) and the phosphane ligand (0.19 mmol)

were dissolved in a minimum amount of tetrahydrofuran in separate flasks. The solutions containing equimolar amounts of Rh(acac)$(CO)_2$ and phosphane (PR_3) were combined and strirred at room temperature overnight. After that, the solution was evaporated to dryness in vacuum. Rh(acac)(CO)(**3**): IR: υ(CO) = 1971 cm^{-1}, $^{31}P\{^1H\}$ NMR: δ_P = 54.6 ppm, $^1J_{P-Rh}$ = 173 Hz. Rh(acac)(CO)(**4**): IR: υ(CO) = 1965 cm^{-1}, $^{31}P\{^1H\}$ NMR: δ_P = 47.0 ppm, $^1J_{P-Rh}$ = 172 Hz, yellow crystals for X-ray studies were grown from dichloromethane. Rh(acac)(CO)(**5**): IR: υ(CO) = 1962 cm^{-1}, $^{31}P\{^1H\}$ NMR: δ_P = 44.1 ppm, $^1J_{P-Rh}$ = 171 Hz. Attempts to crystallize Rh(acac)(CO)(**3**) and Rh(acac)(CO)(**5**) species for further studies were not successful, however.

2.4. Computational details

Gaussian 94 [24] and Sybyl [25] programs were used in modeling. The initial estimation for phosphanes was built on the assumption that the *ortho* substituent was situated outside the cone, otherwise no special geometry around the phosphorus was used. Ligand structures (Scheme 2) were optimized on the HF level of theory using the 3-21G∗ basis set. For the cone angle measurements, the metal(dummy atom)-phosphorus distance 2.28 Å and van der Waals' radius of hydrogen 1.2 Å were used. Initial estimations of the geometries of Rh(acac)(CO)(PR_3) species were based on the solid state structure of Rh(acac)$(CO)_2$ [15,26]. Geometrical optimization of complexes Rh(acac)(CO)(**3**), Rh(acac)(CO)(**4**) and Rh(acac)(CO)(**5**) (Scheme 3) were carried out with the B3PW91 method using the 6-31G∗ basis set.

2.5. X-ray crystallography

The X-ray diffraction data were collected with a Nonius KappaCCD diffractometer using Mo Kα radiation (λ = 0.71073 Å) with a Collect [27] data collection program. The Denzo and Scalepack [28] were used for cell refinements and data reduction. All structures were solved by direct methods using SHELXS97 [29] and the WinGX [30] graphical user interface. A multi-scan absorption correction based on equivalent reflections (XPREP in SHELXTL v. 5.1) [31] was applied to Rh(acac)(CO)(PR_3) (T_{max}/T_{min} = 0.17355/0.10553). Structural refinements were carried out with the SHELXL97 program [29]. The crystallographic data for structures **5** (Fig. 1), **9** (Fig. 2) and Rh(acac)(CO)(**4**) (Fig. 3): are summarized in Table 2 and selected bond lengths and angles in Table 3. Crystallographic data (excluding structural factors) for the structure reported in this paper have been consigned to the Cambridge Crystallographic Data Centre as supplementary publication no. 191946–191948. Copies of the data can be obtained free of charge by request to CCDC, 12 Union Road, Cambridge CB2 1EZ, UK (fax: +44-1223-336-033; e-mail: deposit@ccdc.cam.ac.uk).

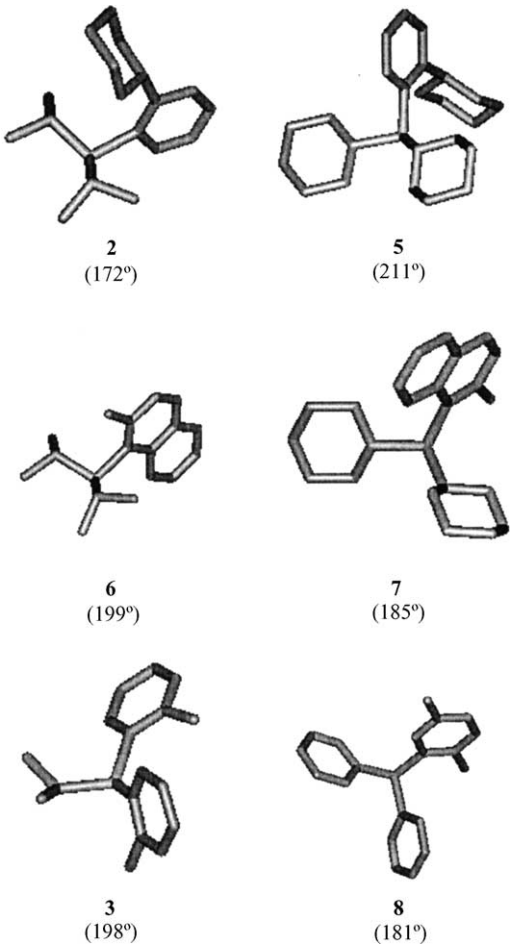

Scheme 2. Gas-phase structures of free ligand; **2**, **5**–**7**, **3** and **8**; and their calculated cone angles.

Scheme 3. Gas-phase structures of complexes Rh(acac)(CO)(**3**), Rh(acac)(CO)(**4**) and Rh(acac)(CO)(**5**).

2.6. Hydroformylation of propene and 1-hexene

The two following procedures were the same for the two alkenes: A disposable inner Teflon reactor was used to avoid the accumulation of rhodium on the reactor walls. The products were analyzed with a Hewlett Packard 5890 GC equipped with a capillary column (HP-1, 1.0 μm × 0.32 mm × 60 m) and a flame-ionization detector. Products were quantified by the internal standard method. In addition, the aldehydes were identified by GC-MS analysis. Conversion, selectivity, and *i*/*n* ratios were calculated on a molar basis. Conversion was calculated with respect to propene (1-hexene) and selectivity with respect to aldehydes. The *i*/*n* ratio of the aldehydes was defined as the amount of branched product divided by the amount of linear product.

Propene hydroformylation: Experiments were carried out in a 250-ml autoclave (Berghof) equipped with a sampling system and a 230-ml Teflon liner. The experiments were done in semibatch mode so that the synthesis gas pressure was kept constant during the experiment. The rhodium precursor was $Rh(NO_3)_3$ (Fluka). In a typical experiment,

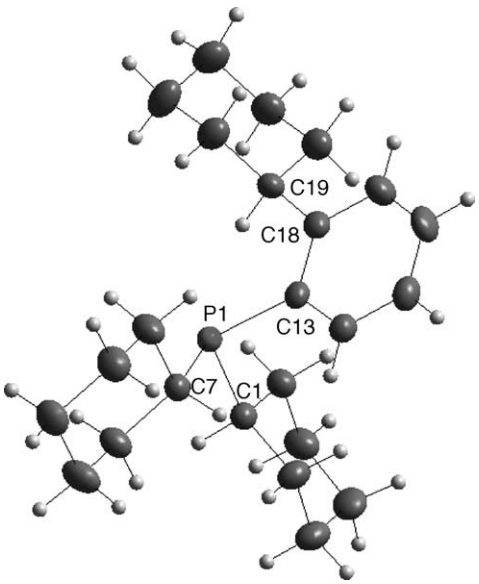

Fig. 1. X-ray crystal structure of (2-cyclohexylphenyl)dicyclohexylphosphane (**5**).

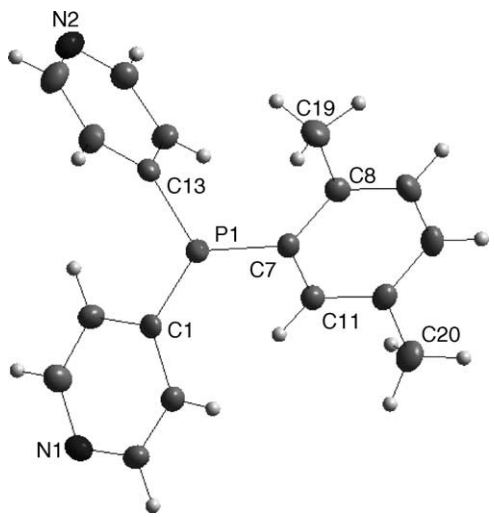

Fig. 2. X-ray crystal structure of (2,5-dimethylphenyl)bis-(4-pyridyl)phosphane (**9**).

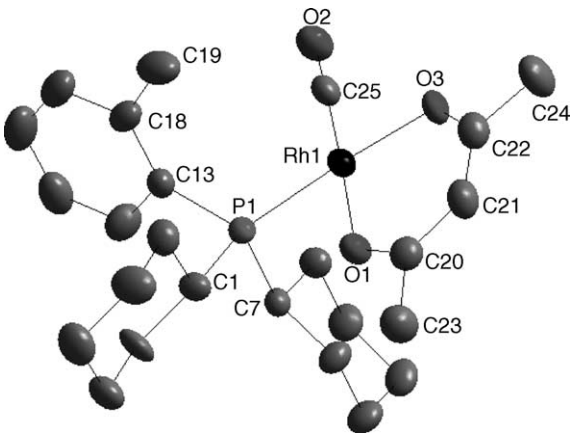

Fig. 3. X-ray crystal structure of complex Rh(acac)(CO)(**4**).

the autoclave was charged with the rhodium precursor (0.02 mmol calculated as rhodium), acetone (310 mmol, Merck, >99%), internal standards decane (7 mmol, Fluka, >98%) and hexane (12 mmol, Riedel de Häen, >99%), and the phosphane. In the case of (2-methylphenyl)dicyclohexylphenylphosphane (**4**) and (2,5-dimethylphenyl)bis(4-pyridyl)phosphane (**9**), THF was used instead of acetone because of solubility problems. The result of (2,5-dimethylphenyl)bis(3-pyridyl)phosphane (**8**) may not be directly comparable with other modified ligands because of different device adjustments. If not otherwise stated, the ligand-to-rhodium ratio was 10:1 on a molar basis. The system was flushed with nitrogen, and pressurized with propene (2 bar, Aga, 99.8%), heated to the reaction temperature (100 °C) with continuous stirring, and then pressurized to the reaction pressure (10 bar) with a 1:1 molar ratio of H_2 and CO (MG, 99.997%).

Table 2
Crystallographic data for structures **5**, **9** and Rh(acac)(CO)(**4**)

	5	**9**	Rh(acac)(CO)(**4**)
Empirical formula	$C_{24}H_{37}P$	$C_{18}H_{17}N_2P$	$C_{25}H_{37}O_3PRh$
F_w (g/mol)	356.51	292.31	519.43
Colour, habit	Bright	Bright	Yellow
Crystal size (mm)	0.40 × 0.40 × 0.30	0.20 × 0.20 × 0.20	0.20 × 0.20 × 0.20
Temperature (K)	150 (2)	150 (2)	120 (2)
Crystal system	Monoclinic	Triclinic	Monoclinic
Space group	*P*2/*c*	$P\bar{1}$	$P2_1/n$
a (Å)	9.1387 (2)	8.8204 (2)	10.0838 (2)
b (Å)	12.4453 (3)	9.9813 (2)	13.1270 (3)
c (Å)	18.9759 (5)	10.5157 (3)	18.3891 (4)
α (°)	90	107.0300 (10)	90
β (°)	96.6355 (9)°	111.6510 (10)°	90.2814 (8)
γ (°)	90	104.928 (2)°	90
Volume (Å^3)	2143.75 (9)	749.87 (3)	2434.14 (9)
Z	4	2	4
ρ (calcd.) (g/ml)	1.105	1.295	1.417
μ (mm^{-1})	0.132	0.178	0.790
Theta range	2.71–25.50	4.18–26.41	2.77–26.00
Index ranges	$-11 \le h \le 11$, $-15 \le k \le 15$, $-22 \le l \le 22$	$-11 \le h \le 10$, $-12 \le k \le 12$, $-13 \le l \le 13$	$-12 \le h \le 10$, $-15 \le k \le 16$, $-20 \le l \le 22$
No. collected reflections	7708	5445	16017
No. unique reflections	3979	3018	4771
R_{int}	0.0202	0.0191	0.0653
R1 ($I \ge 2\sigma$)	0.0396	0.0377	0.0473
wR2 ($I \ge 2\sigma$)	0.0931	0.0936	0.1094
wR2 (all reflections)	0.1008	0.0989	0.1107
Goof	1.045	1.062	1.227

Table 3
Selected bond lengths (Å) and angles (°) for structures **5**, **9** and Rh(acac)(CO)(**4**)

	5	**9**	Rh(acac)(CO)(**4**)
Bond			
P(1)-C(1)	1.865(2)	1.832(2)	1.844(4)
P(1)-C(7)	1.857(2)	1.836(2)	1.848(4)
P(1)-C(13)	1.855(2)	1.835(2)	1.832(4)
C(18)-C(19)	1.520(2)		1.509(7)
C(8)-C(19)		1.511(2)	
C(11)-C(20)		1.508(2)	
P(1)-Rh(1)			2.2510(10)
Rh(1)-O(1)			2.052(3)
Rh(1)-O(3)			2.084(3)
Rh(1)-C(25)			1.795(5)
C(25)-O(2)			1.158(5)
Angle			
C(1)-P(1)-C(7)	103.71(7)	103.35(7)	105.0(2)
C(1)-P(1)-C(13)	102.52(7)	100.90(7)	102.9(2)
C(7)-P(1)-C(13)	102.42(7)	102.68(7)	105.4(2)
C(25)-Rh(1)-P(1)			89.50(13)
O(1)-Rh(1)-C(25)			177.25(15)
O(3)-Rh(1)-P(1)			175.83(9)
Rh(1)-C(25)-O(2)			179.1(4)

At least nine samples were taken for analysis in each experiment: one of the fresh reaction, one immediately after pressurizing with H_2 and CO, which was considered as the starting point of the reaction, six during the experiment, and one after the reaction.

1-Hexene hydroformylation: Experiments were conducted in a 100-ml autoclave (Berghof) with a 60-ml Teflon liner. The experiments were done in batch mode with rhodium precursor Rh(acac)$(CO)_2$. The reactor was charged under a nitrogen purge with substrate, rhodium catalyst, ligand (L/Rh 5), and internal standard, cyclohexane. The autoclave was then sealed and pressurized using a 1:1 mixture of H_2 and CO (MG, 99.997%) to 20 bars and heated at reaction temperature 100 °C for 4 h; the autoclave was then cooled and brought to normal atmospheric pressure.

3. Results and discussion

3.1. Synthesis of free ligands

All the ligands prepared had these essential features. The *ortho*-substituents in the aromatic parts were changed (methyl or cyclohexyl), and the *ortho*-alkyl-substituted aryl rings were combined with alkyl or pyridyl groups instead of phenyl rings. In the preparation of pyridylphosphanes **8** and **9**, we used a combination of low reaction temperatures and the addition of N,N,N′,N′-tetramethylethylenediamine (TMEDA) to prevent addition/coupling reactions during the formation of the pyridyllithium and also to promote a greater reactivity of the pyridyllithium towards the chlorophosphane [22]. Despite this the yields remained rather low especially that of (4-pyridyl)phosphane (12%). Reasonably good yields (76–84%) were obtained for the other ligands studied except for (2-methylphenyl)diisopropylphosphane (35%). The technical grade of 1-bromo-2-methylnaphthalene also lowered the yield of naphthylphosphane ligands (44 and 66%). The ligands are presented in Scheme 1.

3.2. Characterization of free ligands

The structural characterization of the ligands was done by NMR methods. Generally, assignment of the $^{13}C\{^1H\}$ and ^1H chemical shifts were possible. However, due to the overlapping of the ^1H resonances' multiplicities of cyclohexyl groups, substituted phenyl rings and pyridyl rings, the exact peaks remained uninterpreted. The unconfirmed ^1H NMR shifts were assigned on the basis of the information from two-dimensional NMR spectra: H,C-correlated HSQC or C,H-correlated HETCOR, H,H-correlated COSY 90 and long-range C,H-correlated COLOC. Two-dimensional spectra were also necessary in the assignment of the $^{13}C\{^1H\}$ chemical shifts of carbons 3–5 (Table 1, Scheme 1) and the carbons of the naphthyl ring, dicyclohexyl and diisopropyl groups.

According to previous literature, magnetic non-equivalency of protons arises when a group is attached to a center that is asymmetric with respect to the group, although not necessarily with respect to the molecule as a whole, and is manifested as a chemical shift difference between protons that appear to be chemically equivalent [32–34]. The protons may be non-equivalent even if the energy barrier to rotation about the P–C bond is low [32]. We have made the same observation for the *o*-alkyl substituted diisopropylphosphanes (**1**, **2**, **6**) and dicyclohexylphosphanes (**4**, **5**, **7**) studied. In these diisopropylphosphanes and dicyclohexylphosphanes,

the two alkyl groups are equivalent to each other, and the carbon atoms that are symmetrically arranged around the plane of symmetry of each alkyl unit are diastereotopic. The experimental results (Table 1) of ligands **1**, **5** and **6** COLOC-NMR spectra show a long-range ^{13}C-^{1}H ($^{3}J_{CH}$) coupling between non-equivalent carbons 8* and 8** and also 9* and 9**, which is possible only if the two nuclei belong to the same alkyl group. Assignment of ^{13}C chemical shifts of the isopropyl and cyclohexyl carbons agree with the shielding order $\delta(C^{7*}) > \delta(C^{8*})$, $\delta(C^{8**}) > \delta(C^{9*})$, $\delta(C^{9**}) > \delta(C^{10*})$ [33]. Comparison of ^{31}P-^{13}C coupling constants reveals that the diastereotopic carbons are also non-equivalent with respect to P–C coupling constants [32–34]. Both the $^{2}J_{CP}$ and $^{3}J_{CP}$ values of the bond of carbons 8∗∗ and 9∗∗ are considerably larger than those of carbons 8∗ and 9∗. According to previous literature, the two bonds have the same dihedral angle with the P–C bond, only the different average distance to the phosphorus lone pair controls the magnitude of these couplings [33,34]. The phosphorus lone pair is much closer in motional average to the 8∗∗ and 9∗∗ bond than to the 8∗ and 9∗ bond in these compounds [33].

3.3. Synthesis of complexes

Reaction between equimolar amounts of Rh(acac)-$(CO)_2$ and phosphanes (PR_3) afforded rhodium complexes Rh(acac)(CO)(**3**), Rh(acac)(CO)(**4**) and Rh(acac)(CO)(**5**). The isolation of pure complexes was difficult, since the product seems to be in equilibrium with the starting materials. Consequently, only the synthesis of Rh(acac)(CO)(**4**) complex gave a few single crystals after several straight purification operations.

3.4. Ab initio calculations of free ligands and complexes

The cone angles of the free ligands are given in Scheme 1. Compared with triphenylphosphane (149°), the cone angles increased from 165° for **1** to 211° for **5**. Owing to the higher steric repulsion induced by cyclohexyl rings bonded to the phosphorus atom directly (**4**, **5** and **7**), conformations resulted in which the *ortho*-substituents were located outside the cone (see Scheme 2). Optimization of diisopropylphosphanes (**1**, **2** and **6**) led to opposite conformations where *ortho*-alkyl-substituents were located inside the cone. The geometrical arrangement of (2,5-dimethylphenyl)bis(3-pyridyl)phosphane (**8**) resembled dicyclohexylphosphanes. The *ortho*-methyl-substituent lay outside the cone (Scheme 2).

Measurements of the coordinated ligands gave lower cone angle values than the free ligands. The difference was largest in the case of the bis(2-methylphenyl)isopropylphosphane (**3**) ligand. In the free ligand state, the isopropyl group bent inside the cone leaving both methyl groups outside the cone. In the coordinated state, one *o*-methyl substituent was very close to the rhodium center. Consequently, the other methyl group rotated inside the cone, at the same time, the isopropyl group was rotated partly away from the cone. There was a huge difference between the cone angles of the coordinated (163°) and free (198°) states.

In the case of **4** and **5** ligands, methyl and cyclohexyl substituents were similarly bent outside the cone towards rhodium in the free and coordinated state. The substituted benzene ring was only rotated a bit, leaving space for alkyl substituents as the P–Rh bond formed. Consequently, the cone angles of Rh(acac)(CO)(**4**) and Rh(acac)(CO)(**5**) complexes were around 10° smaller than those of the corresponding free ligands.

3.5. Crystal structures of complexe Rh(acac)(CO)(*4*) and ligands *5* and *9*

The structures of both ligands, **5** and **9**, and complex Rh(acac)(CO)(**4**) were determined by single-crystal X-ray diffraction analysis. Crystalographic data are summarized in Table 2 and selected bond lengths and angles are given in Table 3. The crystal structures are shown in Figs. 1–3.

The conformation of (2-cyclohexylphenyldicyclohexylphosphane (**5**) given by ab initio Hartree–Fock calculation (Scheme 1) was similar to that obtained by the X-ray crystal structure measurement (Fig. 1), where the cyclohexyl substituent was located outside the cone. In addition, the conformation of (2,5-dimethylphenyl)bis(3-pyridyl)phosphane (**8**) (Scheme 2) obtained by using the ab initio Hartree–Fock calculation resembled the X-ray crystal structure of (2,5-dimethylphenyl)bis(4-pyridyl)phosphane (**9**) (Fig. 2). Therefore, ab initio Hartree–Fock

Table 4
Results for hydroformylation of propene by rhodium catalysts with reported phosphane ligands

Ligand	θ (°)	δ_P (ppm)	X (%)	Initial rate mol/(mol$_{Rh}$ s)	$S_{isobutanal}$ (%)	i/n
1	165	−4.8	52	17	46	0.9
2	172	−4.4	47	15	48	0.9
3	198	−22.3	22	5	52	1.1
4[a]	181	−11.6	5	0	46	0.9
5	211	−14.6	35	12	49	1.0
6	199	6.6	23	5	35	0.5
7	185	−8.1	22	5	33	0.5
8[b]	181	−25.0	50	15	47	0.9
9[a]	–	−15.7	53	12	48	0.9
PPh_3	149	−3.3	98	45	36	0.6

Reaction conditions: 10 bar (CO/H_2 = 1), T = 100 °C, X: conversion = 2 h, propene/Rh = 512, L/Rh = 10. Initial rate for aldehyde formation.

[a] THF was chosen as a solvent, because of solubility problems. PPh_3: X(2 h) = 81%, r_i = 37, S_i = 36%, THF as solvent.

[b] Different adjustments of the device. PPh_3: X(2 h) = 100%, r_i = 55, S_i = 37%.

calculations were performed for all the ligands studied.

The X-ray crystal structure of Rh(acac)(CO)(**4**) (Fig. 3) was in agreement with the ab initio calculation of the species (Scheme 3). The bond lengths of the X-ray crystal structure and the calculated structure were almost identical: Rh–P bond length, 2.25 Å for crystal structure and 2.30 Å for calculated structure, Rh–C, 1.80 Å for crystal structure and 1.82 Å for calculated structure and the measured C–O bond length was 1.16 Å for both structures. The C–Rh–P angles obtained by using single-crystal X-ray diffraction analysis (89.50°) and by using ab initio calculations (95.36°) were in the same range. The calculated complex structures containing corresponding phosphane ligands seemed to give a reliable qualitative picture of the coordinated state, and thus assisted in the prediction of catalytic activity and selectivity trends.

3.6. Hydroformylation of propene and 1-hexene

Results from the hydroformylation of propene and 1-hexene are displayed in Tables 4 and 5. The widely used triphenylphosphane was chosen as a reference ligand because in the hydroformylation of propene the unmodified rhodium catalyst had very low initial activity and conversion even though isobutanal was formed in a roughly equal amount with *n*-butanal [5].

In the case of 1-hexene hydroformylation, high isomerization activity (>50%) was associated with all ligands, and some hydrogenation activity (<20%) was found as well. In every case, the major isomerization

Table 5
Results for hydroformylation of 1-hexene by rhodium catalysts with reported phosphane ligands

Ligand	θ (°)	δ_P (ppm)	X (%)	$S_{(2-ep)}$ (%)	$S_{(2-mh)}$ (%)	$S_{(1-hep)}$ (%)	i/n
3	198	−22.3	98	1	6	9	0.8
4	181	−11.6	98	0	6	10	0.6
5	211	−14.6	98	3	10	12	1.1
6	199	6.6	99	5	15	15	1.3
7	181	−8.1	98	2	7	9	0.9
8	181	−25.0	98	3	12	14	1.1
PPh_3	149	−3.3	96	0	4	7	0.5
No ligand	–	–	99	5	15	16	1.2

Reaction conditions: 20 bar, T = 100 °C, X = 4 h, 1-hexene 15.5 mmol, $Rh(acac)(CO)_2$ 1.55 × 10^{-6} mol, L/Rh = 5. $S_{(2-ep)}$: selectivity to 2-ethylpentanal; $S_{(2-mh)}$: selectivity to 2-methylhexanal; $S_{(1-hep)}$: selectivity to 1-heptanal.

product was 2-hexene. Nevertheless, the tested ligands **1**–**8** gave higher total aldehyde selectivity and similar conversions comparable with the PPh_3-modified reaction. The main products were 1-heptanal and 2-methylhexanal, respectively.

Generally, the modified phosphanes prepared gave considerably higher *i*/*n* ratios compared with triphenylphosphane. *i*-Selectivity was slightly higher as the size of the *o*-alkyl-substituent became larger with the structure maintained otherwise unmodified. In propene hydroformylation, the enhancement was 2% between diisopropylphosphanes **1** and **2**, and in 1-hexene hydroformylation, 4% between dicyclohexylphosphanes **4** and **5**. In the case of sterically bulkier naphthylphosphane structures **6** and **7**, *i*-selectivity slightly lessened as isopropyls were switched over to cyclohexyl groups; however, with phenylphosphanes, **1**–**5**, no considerable changes appeared. In propene hydroformylation, the *i*/*n* ratios observed with ligands **6** and **7** were even lower than that of the PPh_3 reference. In any case, the best selectivity to total aldehydes (35%) was given by (2-methylnaphthyl)diisopropylphosphane (**6**) in 1-hexene hydroformylation; its regioselectivity to the branched products, 2-methylhexanal and 2-ethylpentanal ($i/n = 1.3$), which was slightly better than when no ligand (1.2) was present. On the whole, the selectivities of the ligands used in this study to form isobutanal were comparable with the previously tested reaction modified with *o*-methyl, *o*-ethyl, *o*-isopropyl and *o*-cyclohexyl substituted phenylphosphanes [5,15].

In propene hydroformylation, the initial activities and conversions of all the *o*-alkyl substituted ligands (5–17 $mol\,mol_{Rh}^{-1}\,s^{-1}$ and 22–52%) studied were considerably lower than that of the PPh_3 ligand (45 $mol\,mol_{Rh}^{-1}\,s^{-1}$, 98%). Relative to the PPh_3, the initial activity of naphthylphosphanes (**6** and **7**) and bis(2-methylphenyl)isopropylphosphane was markedly lower, while that of (2-methylphenyl)diisopropylphosphane was the highest of all synthesized ligands. In the propene hydroformylation reaction, the initial activity and conversion decreased with greater steric crowding of the ligands. With all these ligands, the initial rates and conversions in aldehyde formation were even lower than those with the previously tested phenylphosphanes containing one *o*-methyl, *o*-ethyl, *o*-isopropyl or *o*-cyclohexyl substituted phenyl ring [5,15]. Even pyridylphosphanes **8** and **9** showed lower initial rates compared with the corresponding (2,5-dimethylphenyl)diphenylphosphane although the pyridylphosphane-modified complexes are known to obtain higher reaction rates than their phenyl analogues [15,19,20].

The $^{31}P\{^1H\}$ NMR chemical shifts give information about the stereoelectronic state of the phosphane ligands; whereas, the cone angles are commonly used as a good, but simple measure for steric stress [35]. In addition to the electronegativity, the angles between substituents affect the $^{31}P\{^1H\}$ NMR chemical shifts. It was observed that cone angles became larger and the $^{31}P\{^1H\}$ NMR chemical shifts of the ligands studied became smaller mainly because of the steric stress of the alkyl groups. Closely related ligands showed this approximate order: the *i*-selectivity became greater and initial activity lessened as the $^{31}P\{^1H\}$ NMR shift of the free ligand became less.

4. Conclusions

In the hydroformylation of propene, the conversions and initial rates were negatively affected as the steric demands of the ligands, generated by the *o*-alkyl-substituent of naphthyl or phenyl rings and by alkyl groups bonded to the phosphorus atom directly, became greater. On the other hand, the selectivity in forming isobunal was higher than that of triphenylphosphane. It seemed according to the ab initio HF calculations and single-crystal X-ray studies that one side of the complex was blocked by the alkyl substituent; and thus, the steric properties of the active complex steered the regioselectivity and activity of hydroformylation to the extent that the replacement of isopropyl or cyclohexyl groups with electron-withdrawing pyridyl groups did not change the hydroformylation results notably. On the whole, the *o*-alkyl substituted arylalkylphosphane ligands used in this study were inferior modifiers of rhodium-catalyst to the corresponding *o*-alkyl substituted arylphosphane ligands.

Acknowledgements

We gratefully acknowledge the financial support from Neste Oxo AB and the National Technology

Agency of Finland (Tekes). We wish to thank Ms. Päivi Joensuu and Ms. Sari Ek for the mass spectra and Ms. Merja Harteva for performing the propene hydroformylation tests and Ms. Liisa Saharinen for assistance in the 1-hexene hydroformylation tests and preparation of rhodium complexes.

References

[1] M. Beller, B. Cornils, C.D. Frohning, C.W. Kohlpaintner, J. Mol. Catal. A: Chem. 104 (1995) 17.
[2] A.M. Trzeciak, J.J. Ziülkowski, Coord. Chem. Rev. 190–192 (1999) 883.
[3] B. Breit, W. Seiche, Synthesis 1 (2001) 1.
[4] C.P. Casey, L.M. Petrovich, J. Am. Chem. Soc. 114 (1992) 5535.
[5] H.K. Reinius, P. Suomalainen, H. Riihimäki, E. Karvinen, J. Pursiainen, A.O.I. Krause, J. Catal. 199 (2001) 302.
[6] R.L. Pruett, J.A. Smith, J. Org. Chem. 34 (1969) 327.
[7] P.W.N.M. Van Leeuwen, C.F. Roobeek, J. Organomet. Chem. 258 (1983) 343.
[8] A. Van Rooy, E.N. Otij, P.J.C. Kamer, F. van den Aardweg, P.W.N.M. van Leeuwen, J. Chem. Soc., Chem. Commun. (1991) 1096.
[9] A. Van Rooy, E.N. Orij, P.C.J. Kamer, P.W.N.M. Van Leeuwen, Organometallics 14 (1995) 34.
[10] T. Jongsma, G. Challa, P.W.N.M. van Leeuwen, J. Organomet. Chem. 421 (1991) 121.
[11] N. Poelsma, P. Maitlis, J. Organomet Chem. 451 (1993) C15.
[12] B. Cornils, W.A. Herrmann, Applied Homogenous Catalysis with Organometallic Compounds, vol. 1, VCH, Weinheim, 1996, Chapter 2, pp. 58–59.
[13] A.A. Oswald, J.S. Merola, J.C. Reisch, R.V. Kastrup, US Patent, WO 84/03697 (1984).
[14] F. Ancilotti, M. Lamiand, M. Marchionna, J. Mol. Catal. 63 (1990) 15.
[15] H. Riihimäki, P. Suomalainen, H.K. Reinius, J. Suutari, S. Jääskeläinen, A.O.I. Krause, T.A. Pakkanen, J.T. Pursiainen, *o*-Alkyl-substituted aromatic phosphanes for hydroformylation studies: synthesis, spectroscopic characterization and ab initio investigations, J. Mol. Catal. A: Chem. 200 (2003) 69–79.
[16] A.A. Oswald, D.E. Hendriksen, R.V. Kastrup, E.J. Mozeleski, Adv. Chem. Ser. 230 (1992) 395.
[17] A.A. Oswald, D.E. Hendriksen, R.V. Kastrup, K. Irikura, E.J. Mozeleski, D.A. Young, Phosphorus Sulfur 30 (1987) 237.
[18] P. Suomalainen, H. Riihimäki, S. Jääskeläinen, M. Haukka, J.T. Pursiainen, T.A. Pakkanen, Catal. Lett. 77 (2001) 125.
[19] A. Buhling, P.C.J. Kamer, P.W.N.M. Van Leeuwen, J. Mol. Cat. A: Chem. 98 (1995) 69.
[20] A. Buhling, J.W. Elgersma, S. Nkrumah, P.C.J. Kamer, P.W.N.M. van Leeuwen, J. Chem. Soc., Dalton Trans. (1996) 2143.
[21] G. Dyer, D.W. Meek, J. Am. Chem. Soc. 89 (1967) 3983.
[22] R.J. Bowen, A.C. Garner, S.J. Berners-Price, I.D. Jenkins, R.E. Sue, J. Organomet. Chem. 554 (1998) 181.
[23] B. Buchner, L.B. Lockhart, J. Am. Chem. Soc. 73 (1951) 755.
[24] M.J. Frish, G.A. Petersson, J.A. Montgomery, K. Raghavachari, M.A. Al-Lahman, V.G. Zakrzewski, J.V. Ortiz, J.B. Foresman, J. Ciolowski, B.B. Stefanov, A. Nanayakkara, M. Challacombe, C.Y. Peng, P.Y. Ayala, W. Chen, M.W. Wong, J.L. Andres, E.S. Replogle, R. Gomperts, R.L. Martin, D.J. Fox, J.S. Binkley, D.J. Defrees, J. Baker, J.P. Stewart, M. Head-Gordon, C. Gonzales, J.A. Pople, Gaussian Inc., Pittsburgh PA, 1995.
[25] Sybyl 6.03, Tripos Associates, 1699 S. Hanley Road, Suite 303, St. Louis, MO 63144.
[26] F. Huq, A.C. Skapski, J. Cryst. Mol. Struct. 4 (1974) 411.
[27] *Collect* Data Collection Software, Nonius B.V., 1997–2000.
[28] Z. Otwinowski, W. Minor, Processing of X-ray Diffraction Data Collected in Oscillation Mode In Methods, in: C.W. Carter Jr., R.M. Sweet (Eds.), Enzymology, vol. 276, Macromolecular Crystallography, Part A, Academic Press, New York, 1997, pp. 307–326.
[29] G.M. Sheldrick, SHELXS97, Program for Crystal Structure Determination, University of Göttingen, 1997.
[30] L.J. Farrugia, J. Appl. Cryst. 32 (1999) 837.
[31] G.M. Sheldrick, *SHELXTL* Version 5.1, Bruker Analytical X-ray Systems, Bruker AXS, Inc. Madison, Wisconsin, USA, 1998.
[32] W. McFarlane, Chem. Commun. (1968) 229.
[33] J. Schraml, M. Èapka, V. Blechta, Magnet. Reson. Chem. 30 (1992) 544.
[34] J. Schraml, V. Blechta, E. Krahé, Collect. Czech. Chem. Commun. 57 (1992) 2005.
[35] C.A. Tolman, Chem. Rev. (1976) 313.